THE AMERICAN SOCIETY OF MECHANICAL ENGINEERS
Three Park Avenue, New York, N.Y. 10016-5990

99-GT-290

THREE-DIMENSIONAL PERFORMANCE PREDICTION OF MULTISTAGE AXIAL FLOW COMPRESSORS WITH A REPEATING STAGE MODEL

Y.G.Li **A.Tourlidakis** **R.L.Elder**

School of Mechanical Engineering
Cranfield University
Bedfordshire MK43 0AL, UK

ABSTRACT

In this paper, a method for the performance prediction of multistage axial flow compressors through a steady, three-dimensional, multi-block Navier-Stokes solver is presented.

A repeating stage model has been developed aiming at the simplification of the required global aerodynamic boundary conditions for the simulation of the rear stages of multistage axial compressors where only mass flow rate and exit average static pressure are required. The stage inlet velocity distribution is fixed to be equal to the one calculated at the stage exit and the exit static pressure distribution is fixed to have the same shape to that at inlet but maintain its own average value. A mixing plane approach is used to exchange information between neighbouring blade rows which allows both radial and circumferential variations at both sides of the interface.

A pressure correction method with the standard $k-\epsilon$ turbulence model is used in combination with Stone's two step procedure for the solution of the algebraic system of the discretised equations. A global iteration is carried out in order to establish the physical consistency between the blade rows.

A combination of two structured grid blocks for the rotor blade row, one for the main passage and a second for the modelling of the tip clearance, is used for a detailed representation of the leakage flows.

Computational results from two methods, the first by using the repeating stage model and the second by setting stage inlet velocity profile, are presented from the analysis of the third stage of the four-stage Cranfield Low Speed Research Compressor (LSRC). Good agreements with the experimental data are obtained in terms of total pressure, static pressure and velocity distributions at the inlet, exit and interface planes proving that the repeating stage model is a very economical and accurate alternative to the very expensive complete multistage simulations.

NOMENCLATURE

A, B	matrix coefficients
C	scaling factor
C_{p_t}	$(P_t - P_{ref})/(\frac{1}{2}\rho U_m^2)$
G	production rate of turbulent kinetic energy
J	Jacobian of the Transformation
P	pressure
S	source term
U_m	midspan blade speed
V, W	absolute and relative velocities
$V^j, j = 1,2,3$	contravariant velocity components
c_μ, c_1, c_2	$k-\epsilon$ model coefficients
g^{ij}	contravariant base matrix
k	kinetic energy
$\dot{m}$	mass flow rate
$\vec{u}$	Cartesian velocity vector
$u_i, i = 1,2,3$	Cartesian velocity components
Γ	diffusion coefficient
Φ	solution variable
ρ	density
ϵ	turbulent energy dissipation
ω	rotational speed; under relaxation factor
ν_t	eddy viscosity
$\xi^j, j = 1,2,3$	body-fitted computational coordinates

Presented at the International Gas Turbine & Aeroengine Congress & Exhibition
Indianapolis, Indiana — June 7–June 10, 1999

Superscripts

(n)	iteration level
$*$	provisional quantity
$'$	correction

Subscripts

a	axial
c	circumferential
cal	calculated
$exit$	stage exit
r	radial
ref	reference
p	central node
s	static
t	stagnation
Φ	quantity associated with variable Φ

INTRODUCTION

The flow field in a multistage axial compressor is extremely complicated and can be described as being unsteady, three-dimensional and highly viscous. Computational fluid dynamics (CFD) has been used to predict the flow field in axial flow compressors and computational methods simulating flows in isolated compressor blade rows are highly developed and commonly used in design processes. This class of methods can predict the flow phenomena within isolated blade rows quite successfully once the upstream and downstream boundary conditions are specified correctly. However, few axial flow compressors operate as a series of isolated blade rows. Most axial flow compressors include several stages in order to achieve high pressure ratios. The difficulties of multistage simulation lie in how to cope with the unsteadiness of the absolute flow due to the relative motion between successive blade rows, and how to satisfy the continuity of mass, momentum and energy throughout the whole machine.

In multistage axial flow compressors it is observed that the flow features repeat after several stages from the entry to the exit of the stage while the annular turbulent boundary layer get fully developed. This phenomenon was analysed numerically with Navier-Stokes solvers for two repeating stage compressors, Bolger and Horlock, 1995. The repeating nature of the flows within the multistage environments were well predicted by modelling closely the inlet and exit boundary conditions especially to simulate the measured static pressure fields.

Several methods have been developed for multistage turbomachinery simulation and may be categorised as follows (Chima et al., 1998). The first one is the successive analysis of isolated blade rows where an analysis code for an isolated blade row is available. This method is simple but is difficult to accurately define the boundary conditions and match the spanwise distributions of properties between blade rows and in addition ignores a lot of physical processes that may be important in real turbomachines. This method was used by several researchers, such as Boyle et al., 1995 and Politis et al., 1997. The second type is mixing-plane methods introduced simultaneously by Denton, 1992 and Dawes, 1992, where spanwise consistency is maintained between the blade rows although some physics may be missed. Adamczyk et al., 1984 introduced an average-passage method to take into account unsteady blade row interaction by using steady state methods. This method and the corresponding code NASTAR developed by Rhie et al., 1995 were applied successfully to the design of a P&W's eleven stage high pressure compressor (LeJambie et al., 1995). This approach is more rigorous than mixing-plane methods and also more complicated to use in terms of programming and computation. Another type is fully unsteady methods, pioneered by Rai, 1989, which could be used to simulate flow phenomena accurately and avoid all modelling questions except for turbulence. However, fully unsteady methods are still too expensive computationally especially when being applied in multistage environments.

In this paper, a multistage turbomachinery simulation method and a code MSTurbo3D, which is developed from an analysis code ELISA for isolated blade row (Politis et al., 1997) is described. An improved circumferential non-uniform mixing-plane technique (Denton, 1992) is used to pass information and keep spanwise consistency for static pressure, velocity, k and ϵ profiles between neighbouring blade rows and allow the mixing planes to be located close to the leading or trailing edges of blades. A repeating stage model has been developed and used in the simulation, which has the advantage that only mass flow rate and exit average static pressure are necessary as global aerodynamic input. A two-block grid system offers detailed flow description in the clearance region of the rotor. A pressure correction method is used to solve the three-dimensional, incompressible, Navier-Stokes equations.

Finally, results from two computations are presented for the third stage of Cranfield Low Speed Research Compressor (LSRC) operating at peak efficiency, one for the case where the repeating stage model was utilized and another for the case where the inlet velocity profile was fixed from experimental data. A two-block grid with totally 118,875 grid points for the rotor and a single block grid consisting of 91,875 grid points for the stator were used in the computation. A comparison between numerical results and experimental data is provided.

GOVERNING EQUATIONS

For three-dimensional, steady, incompressible, turbulent

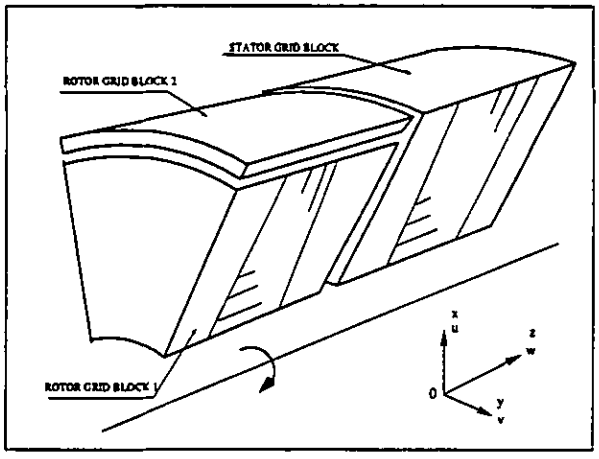

Figure 1: Grid Block Arrangement (Politis et al., 1997)

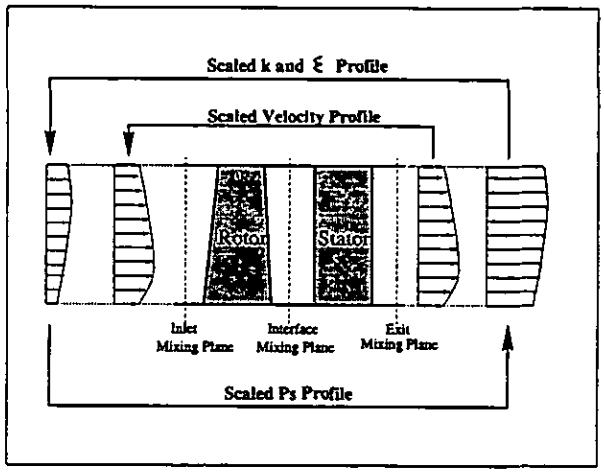

Figure 2: Repeating Stage Model

flows in low speed axial compressors, the governing equations are the continuity and momentum equations in their Reynolds averaged forms. The standard two-equation $k-\epsilon$ turbulence model (Launder and Spalding, 1974) is introduced to "close" the Reynolds averaged Navier-Stokes equations. The near wall region are modelled through the use of the standard wall function approach (Launder and Spalding, 1974).

In order to cope with complex geometries, a non-orthogonal curvilinear coordinate system $\xi^i, i = 1,2,3$, is built and the transformed governing equations are expressed in the following forms:

$$\frac{\partial}{\partial \xi^j}(JV^j) = 0 \tag{1}$$

$$\frac{\partial}{\partial \xi^j}(JV^j\Phi) = \frac{\partial}{\partial \xi^j}(J\Gamma^\Phi g^{jk}\frac{\partial \Phi}{\partial \xi^k}) + JS^\Phi \tag{2}$$

where Φ stands for $u_i, i = 1,2,3$, in stationary or rotating frames of reference, k and ϵ.

In the momentum equations, the source term $S^{\vec{u}}$ includes the effective pressure gradients, all the other terms $\vec{C}$ not included in the diffusion term of Equation 2 and Coriolis and centrifugal forces if in rotating frame, which may be written in the following forms:

$$S^{\vec{u}} = -\frac{1}{\rho}\nabla(P + \frac{2}{3}\rho k) + \vec{C} - 2\vec{\omega}\otimes\vec{W} - \vec{\omega}\otimes(\vec{\omega}\otimes\vec{r}) \tag{3}$$

The source terms in $k-\epsilon$ equations are as follows:

$$S^k = G - \rho\epsilon \tag{4}$$

$$S^\epsilon = (C_1 G - C_2\rho\epsilon)\frac{\epsilon}{k} \tag{5}$$

The Bousinesq hypothesis is introduced to link the turbulent viscosity ν_t with k and ϵ:

$$\nu_t = c_\mu \frac{k^2}{\epsilon} \tag{6}$$

GRID SYSTEM

In order to simulate flow patterns in different flow domains more accurately, a two-block H-type grid for the rotor and a single H-type block grid for the stator are used. In the rotor passage including upstream and downstream extensions, the first block fills the main passage below the cylindrical blade-to-blade surface at the blade tip radius and the second block fills the remaining part of the flow domain including the tip clearance area, which was described in detail by Politis et al., 1997. In the stator passage, a single block is used to describe the domain between two shrouded stator blades including upstream and downstream extensions (see Figure 1).

Three-dimensional surface fitting is based on the idea of Coons patches (Coon, 1967) where a relation is generated between parametric planes and physical surfaces of blade defined by sets of discrete networked points. A set of polynomial functions are used to construct the Ferguson surface patches (Faux and Pratt, 1979) which define the three-dimensional blade surfaces and create boundary grid points. Subsequently, an algebraic grid generation technique including grid point clustering, are used to generate the interior grid points. This set of grid generation tools is relatively simple, but very fast and effective.

REPEATING STAGE MODEL AND BOUNDARY CONDITIONS

It has been observed that in multistage compressors a repeating flow pattern develops after several stages where the turhulent boundary layers on the hub and shroud walls are fully developed. This repeating nature, for the incom-

pressible flows in the particular case concerned, includes unchanged spanwise profiles of velocity, k and ϵ and unchanged patterns of static and total pressure at the inlet and exit of the rear stages. It is assumed that each rear stage of a multistage axial flow compressor is quite like a repeating stage of its neighbouring stages. This assumption results in the repeating stage model that can be used in flow simulations. It has the advantages that the inlet velocity profile becomes the result of the simulation rather than inlet boundary condition and only the average static pressure downstream of the stage together with total mass flow rate are required as global input.

Figure 2 shows how the repeating stage model is implemented. For a typical rear stage of a multistage axial flow compressor there are three mixing planes used to pass tangentially area-averaged information between neighbouring blade rows, one at the inlet of the stage located midway between the current rotor and upstream stator, one at the interface of the stage concerned and another at exit of the stage located midway between the current stator and downstream rotor.

It is assumed that the spanwise velocity profile at inlet is set to be simillar to that at stage exit. The total mass flow rate is used to scale the inlet velocity profile in order to maintain mass continuity during global iterations. The velocity scaling factor C_v is calculated as:

$$C_v = \frac{\dot{m}}{\dot{m}_{cal}} \tag{7}$$

where $\dot{m}$ is the defined mass flow rate and $\dot{m}_{cal}$ is the calculated mass flow rate by imposing the stage exit velocity profile at the stage inlet. The three velocity components, axial, tangential and radial velocity components, are scaled using the same scaling factor in order to keep the absolute flow angle unchanged after scaling. The scaling factor becomes unity when global convergence is achieved.

Similarly, the inlet k and ϵ profiles are set to be equal to those at stage exit as they tend to be unchanged when the turbulent flow is fully developed, and hence the scaling factors for k and ϵ profiles are equal to 1.

The way of setting the static pressure at exit of the stage concerned is to define the average static pressure for the whole exit area as a given value but allow pressure variation to exist radially and circumferentially. Firstly, it is supposed that the static pressure at each point of the exit plane is equal to its upstream value. Then the static pressure at exit is scaled by a scaling factor C_{p_s}:

$$C_{p_s} = \frac{P_{exit}}{P_{cal}} \tag{8}$$

where P_{exit} is the specified value of average static pressure at the stage exit, P_{cal} is the calculated area-averaged static

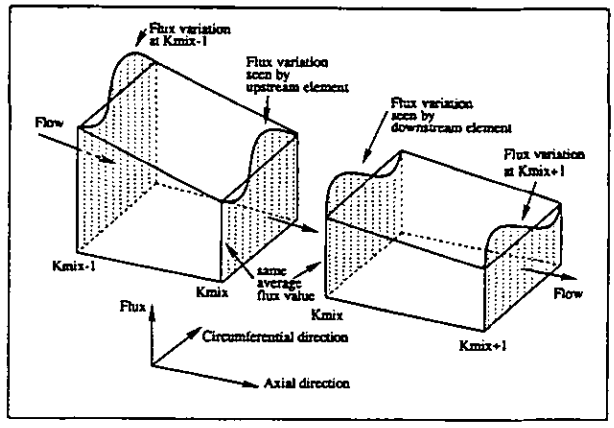

Figure 3: **Mixing-Plane Model (Denton, 1992)**

pressure at the stage exit after imposing the closest upstream pressure field at the exit. This kind of setting also results in the similarity of radial total pressure distribution at inlet and exit of the stage because the flow is supposed to be incompressible and the total pressure is calculated using static pressure and velocity values.

The above model is based on the particular case concerned, where the compressor has constant inner and outer diameters and the flow is supposed to be incompressible. In the general case, if the compressor annulus is convergent downstream and the flow is compressible, the current repeating stage model needs to be further modified. This issue will not be discussed in this paper.

Two methods were introduced for the setting of the aerodynamic boundary conditions. The first method uses the repeating stage model. The second one defines the boundary conditions in the conventional way based on the experimental data, which is straightforward but relies on the available experimental data.

A Neumann boundary condition is imposed on velocity at exit and pressure at inlet of the stage. On all solid surfaces, a noslip condition is used for velocity and a zero gradient condition for pressure is implemented. Periodic conditions are applied on hoth sides of upstream and downstream blade extensions. The cylindrical interface between two blocks is treated by means of halo cells extended from one block into the interior of the adjacent one. Interpolation is used to exchange information between the two blocks.

MIXING PLANE MODEL

In order to calculate flows inside multistage blade rows through a steady state modelling approach, frames of reference are fixed on rotating blades for rotors and stationary blades for stators. Hence, difficulties arise on how to pass information between the two frames which are in relative

motion and maintain consistency of variables at the interfaces.

The circumferential non-uniform mixing-plane method introduced by Denton, 1992, is adopted in the present study, Figure 3. Firstly, a common surface midway between two neighbouring blade rows is chosen as a mixing-plane which is the exit surface of the downstream extension of the upstream blade row and the inlet surface of the upstream extension of the downstream blade row. Then extrapolation is used to provide values of the variables at the mixing plane from upstream or downstream points of the same blade row. Subsequently, area averaging is used to obtain fluxes for different variables at different radial positions on both sides of the mixing plane. Finally, the fluxes on both sides of the mixing plane are forced to be equal by scaling, according to the propagating direction of the information and the ratios of fluxes on both sides of the plane. In the current code MSTurbo3D, the spanwise and circumferentially non-uniform pressure profile propagates upstream and the radial velocity profile and other information downstream, sharing the same fluxes at mixing planes. This model has the advantage that both radial and circumferential variation exist on both sides of the mixing plane, the consistency of mass, static pressure and velocity at interface is guaranteed and the position of the mixing planes are allowed to be located close to the leading or trailing edges of the blade rows with little influence on blade loading. Unfortunately, although mass continuity is conserved automatically because of the area averaging method used, the continuity of momentum, total pressure, total temperature etc. are not guaranteed when information is passed across mixing planes. The influence of these discontinuities may not be an important issue for the prediction of certain stages at peak efficiency. However, at conditions nearer to stall where separations become important, the errors introduced by this approach may grow rapidly.

NUMERICAL PROCEDURES

The flow passage is covered by control volumes and all variables are stored at the centre of these control volumes. The governing equations are discretised at each control volume by using central difference for the diffusion terms, and the QUICK scheme (Leonard, 1979) for the convection terms in the momentum equations and the first-order upwind scheme for the same terms in the k and ϵ equations. As a result, five semi-implicit differential equations incorporating the centre and its six adjacent nodes are formed for each control volume .

All equations are under-relaxed and the discretised equations have the form:

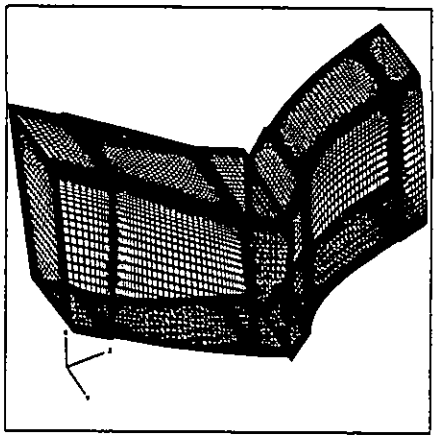

Figure 4: **Grid Layout**

$$-\frac{A_p}{\omega}\Phi_p^* + \sum_k A_k\Phi_k^* + S^{(n)} + \frac{1-\omega}{\omega}A_p\Phi^{(n)} = 0 \qquad (9)$$

where P stands for the central node and the summation symbol incorporates its six direct neighbours. ω is the relaxation parameter; the value $\omega = 0.3$ is normally used and this value is reduced when there is a small separation in the flow field.

The pressure correction scheme (Patankar et al., 1972) is employed to update the velocity field $(u_i, i = 1,2,3)$ resulted from the solution of momentum equations and the pressure field $P^{(n)}$ of the previous iteration in order to satisfy the continuity equation.

$$u_i^{(n+1)} = u_i^* + u_i'(P'^*) \qquad (10)$$

$$P^{(n+1)} = P^{(n)} + P'^* \qquad (11)$$

The pressure correction equation is deduced by introducing Equations 9, 10 and 11 into the discretised contiuity Equation 1 and obtains the following form:

$$-\frac{B_p}{\omega}P_p'^* + \sum_k P_k'^* - S_p^* + \frac{1-\omega}{\omega}B_pP_p'^{(n)} = 0 \qquad (12)$$

where S_p^* stands for the divergence of the provisional velocity field and the summation symbol is used as in Equation.9.

The incomplete decomposition of the coefficient matrix of Equations 9 and 12 into upper and lower matrices is carried out by using Stone's formula (Stone, 1965). After the unique matrix inversion, the dependent variables are obtained using a two-step procedure to obtain a provisional velocity field $u_i^*, (i = 1,2,3), k^*$ and ϵ^* fields and the pressure correction variable P'^* which is used afterwards to make corrections to the provisional velocity field and the pressure field hy using Equation.10 and 11.

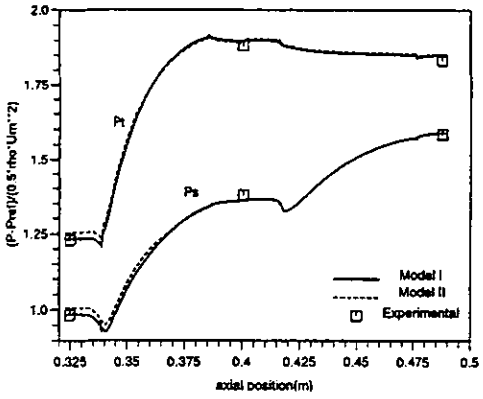

Figure 5: **Pt & Ps in Axial Direction**

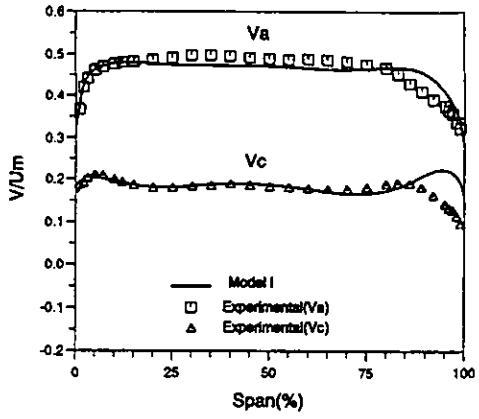

Figure 6: **Spanwise Velocities at Rotor Inlet**

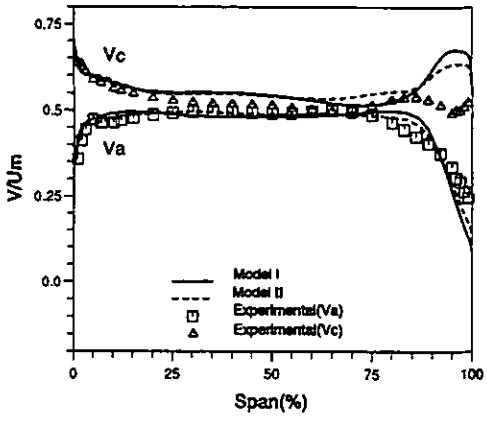

Figure 7: **Spanwise Velocities at Interface**

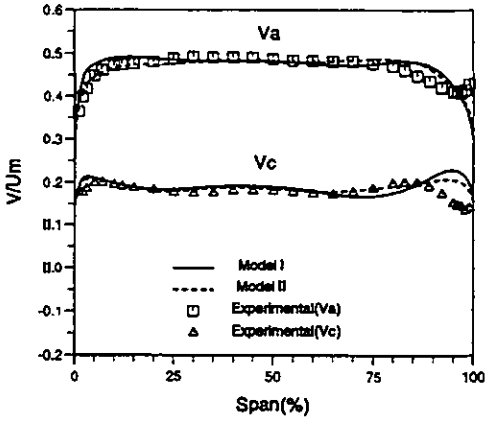

Figure 8: **Spanwise Velocities at Stator Exit**

For multistage turbomachinery simulation, the more stages involved the more difficult the simulation will be. In order to achieve a converged solution, two types of convergence criteria must be satisfied. The first one refers to the numerical convergence criterion for the governing equations on each blade row, which is satisfied when the residuals of all the governing equations are sufficiently small. The second type is the physical convergence criterion for the global iterations when physical flow quantities of the flow (mass flow rate, velocity, static and total pressure) stop changing providing consistency at the interfaces between blade rows with global iteration count. Specified target mass flow rate for each blade row as a constraint and under-relaxation are used globally to enhance effectively the global convergence.

Parameter	Rotor	Stator
Mass flow rate (kg/s)	12.04	12.04
Rotating Speed (rpm)	1100	1100
Tip Clearance (t/h)	2.0%	0.0%
Number of Blades	75	96
Aspect Ratio	1.36	1.36
Space/Chord	0.71	0.55
Max. Thickness Chord	0.095	0.088
Turning (deg)	15.7	26.7
Exit Whirl (rel) (deg)	42.8	20.5
Diffusion Factor	0.42	0.41
Grids	35x35x75(main) 40x9x75 (tip)	35x35x75
Node Number	118,875	91,875

Table 1: **Details of LSRC Third stage**

APPLICATION AND ANALYSIS

In principle, there is no limit to the number of stages concerned for the simulation in a single run and the only limits are the availahle computer resources. As an application, the code MSTurbo3D was used for the internal flow and performance simulation of the third stage of Cranfield

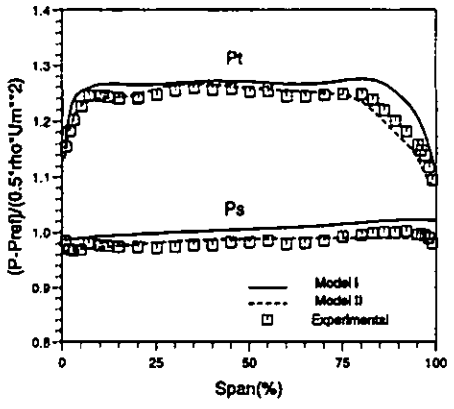

Figure 9: **Spanwise Pressures at Rotor Inlet**

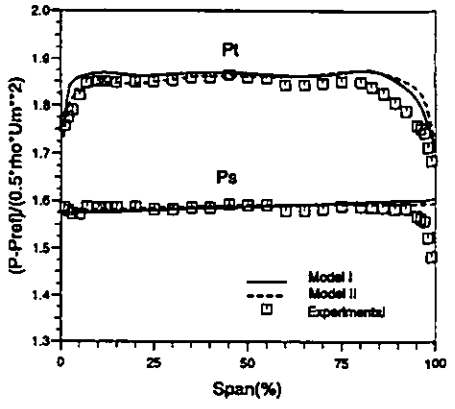

Figure 11: **Spanwise Pressures at Stator Exit**

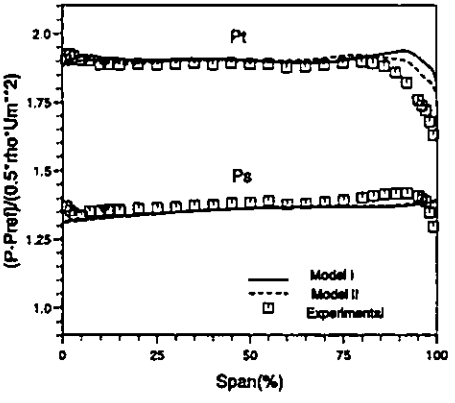

Figure 10: **Spanwise Pressures at Interface**

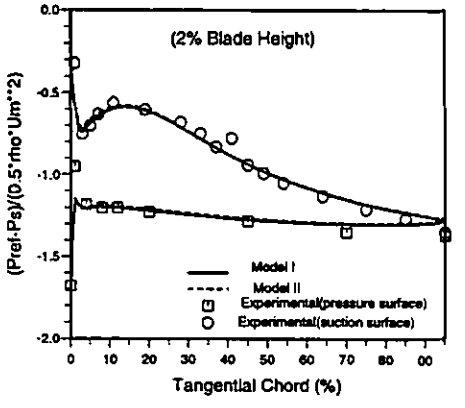

Figure 12: P_s **on Rotor Hub Surface**

University (CU) 4-stage Low Speed Research Compressor (LSRC) whose blading design is reported by Swoboda et al., 1996. The experimental data were obtained during the Advanced Civil Compressor Aerodynamics (AC3A) project (Swoboda et al., 1998). The compressor consists of four repeating stages which are designed to be representative of the rear stages of a high pressure compressor where tip leakage effects play a dominant role. The main characteristics and grid details of the third stage are presented in Table 1.

In the case concerned, a two-block grid with a total of 118,875 nodes is used in the rotor to take into account the tip clearance effect and a single block grid with 91,875 nodes is used in the stator with shrouded blades. The layout of the grids is shown in Figure 4.

The computational time requirement for each inner iteration is approximately 5 seconds on a DEC ALPHA FARM. Typically, a maximum number of 5,000 inner iterations is used locally for each blade row to satisfy numerical convergence criteria for the governing equations and about 15 global iterations are required for global convergence.

Performance comparisons of the third stage of LSRC are carried out at the operating point of peak efficiency, at the inlet, the exit and the interface between the blade rows in terms of total pressure, static pressure and velocity components, and on two blade surfaces at blade hub, midspan and tip in terms of static pressure, based on the available experimental data from the AC3A project (Swoboda et al., 1998) where total pressure, static pressure and flow angle distributions were directly measured whereas velocity components were calculated from them.

Two different calculation methods were used and detailed comparisons between computational results and experimental data were carried out. In the first case which is named as Model I, the repeating stage model is implemented for the definition of the inlet velocity, k and ϵ and exit average static pressure. The main advantage of this model is the simplification of the global aerodynamic boundary conditions where no specified inlet velocity profile is required. However, the successful application of the model relies on whether the stages themselves physically present repeating flow characteristics. The second computational method, named as Model II, is carried out by setting aerodynamic

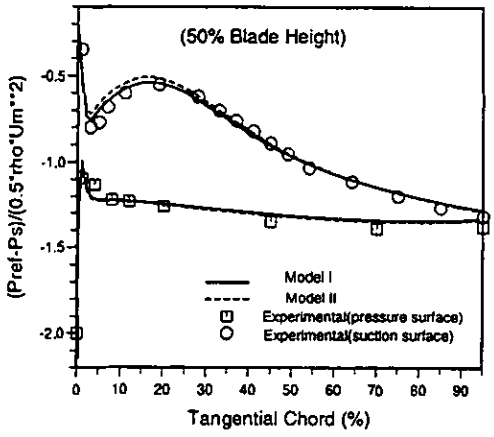

Figure 13: P_s on Rotor Midspan Surface

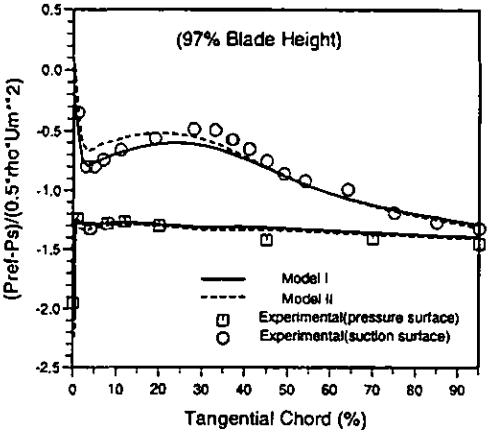

Figure 14: P_s on Rotor Tip Surface

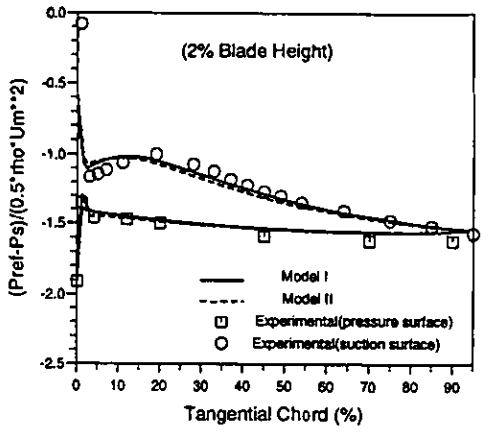

Figure 15: P_s on Stator Hub Surface

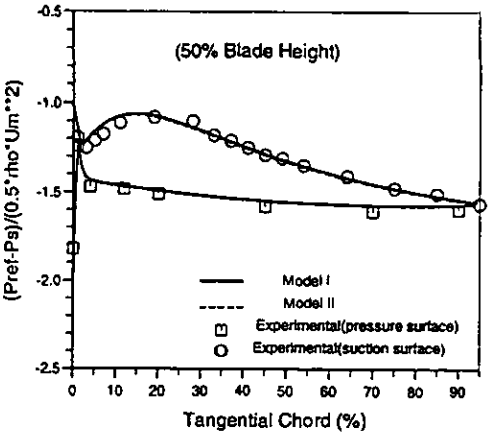

Figure 16: P_s on Stator Midspan Surface

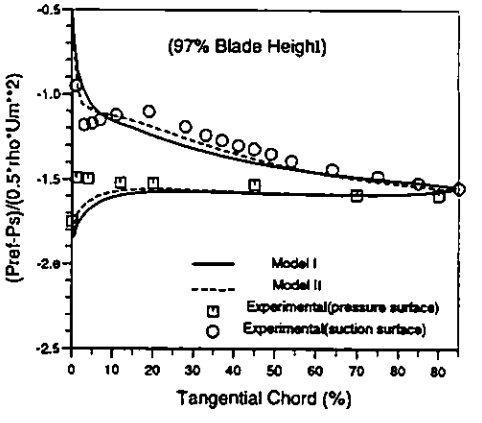

Figure 17: P_s on Stator Tip Surface

boundary conditions based on the experimental data.

The predicted area averaged static pressure and total pressure distributions in the axial direction of the third stage are presented in Figure 5. Compared with experimental data at three stations, the inlet, the interface between the two blade rows and the exit, good agreement between computational and experimental data is shown in the figure although there are small discrepancies. When average static pressure is fixed at stator exit, about 2% over-predicted static pressure ratios were predicted in the stator from both models. For the rotor, 4% under-predicted static pressure ratio from Model I and 2% from Model II were found. The static pressure ratio from Model I was under-predicted as compared to Model II because the inlet velocity profile used in Model I was not exactly the same to the experimental data. Regarding total pressure, Model II offers good prediction for total pressure ratios in both rotor and stator but with around 2% over-predicted absolute values, whereas Model I offers accurate total pressure value at the rotor inlet although with a slightly over-estimated total pressure ratio for the rotor. Sudden changes on average

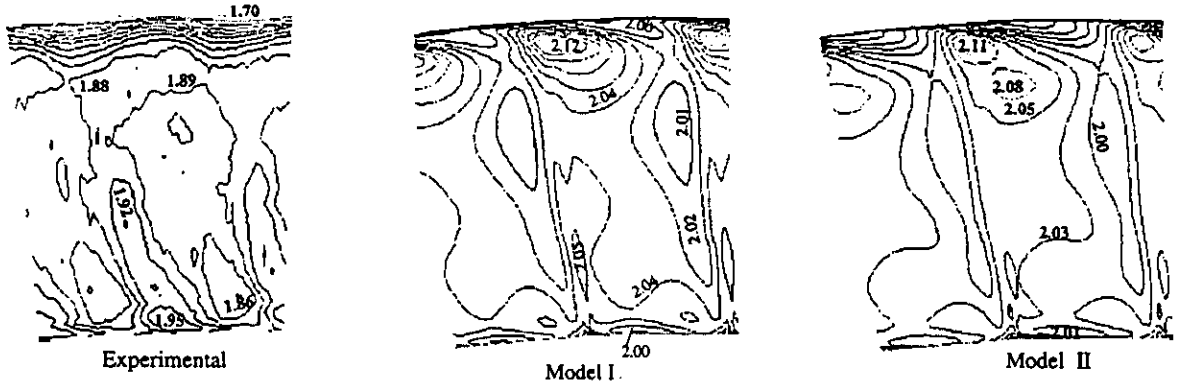

Figure 18: C_{P_t} **Contour at Rotor Exit**

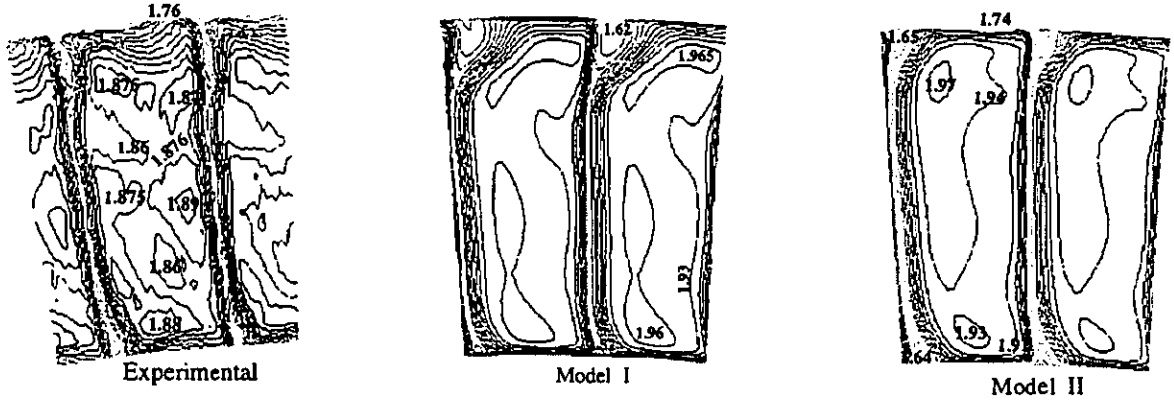

Figure 19: C_{P_t} Contour at Stator Exit

static pressure and total pressure appear near the leading and trailing edges of the blade rows.

The difference between the total pressures on both sides of the mixing plane is nearly negligible, showing that the discontinuity of the momentum resulted from the mixing-plane model is very small and can be neglected at peak efficiency for this particular case.

The calculated spanwise distribution of velocity components from both models at the rotor inlet (except for Model II at this station), the interface between the two blade rows and the stator exit match very well with the experimental data for most part of the blade span although with some discrepancies in the area between 80% and 100% span near the rotor tip, see Figure 6 to 8. These discrepancies are very likely due to numerical inaccuracies in resolving the complex, unsteady tip clearance region because even when the inlet velocity profiles are set equal to the experimental data in Model II these discrepancies still exist.

In Figures 9 to 11 the spanwise distribution of static and total pressure are presented for the three planes. Both models give good predictions for static pressure at the three stations, except for the over-estimated average value at rotor inlet for Model I that can also be observed in Figure 5. This over-estimation of static pressure at rotor inlet also contributes to the over prediction of total pressure at the same area, Figure 9. The sudden changes of experimental static pressure near the walls are not physical and susceptible to measurement error due to the presence of the solid walls (Howard et al., 1994). Hence, the difference in static pressure between experiment and prediction near the blade tip should not be as large as shown in Figures 10 and 11.

The spanwise total pressure distributions are well-predicted for both models as compared with experimental data except for the area between 80% and 100% span. In the case concerned where the compressor is a low speed research compressor, the flow is assumed to be incompressible and the total pressure is calculated using static pressure and velocity values so the discrepancy of total pressure near the

blade tip is caused by the inaccurate prediction of velocity distribution in this area.

Static pressure distributions on both rotor and stator blade surfaces are compared in Figures 12 to 17 and show very good agreement between computational and experimental data for most stations. Some discrepancies in the static pressure values near the stator blade leading edge are shown in Figure 17, which may due to the inaccurate prediction of rotor tip leakage flow and the subsequent inaccurate flow incidence to the stator near the blade tip.

The predicted total pressure contours at the rotor and stator exit planes in terms of C_{p_t} are plotted and compared against the corresponding experimental contours. In Figure 18, both models predict clear wakes at downstream of rotor and large pressure gradients near the blade tips. The predicted tangential gradients are in agreement with the experimental contours but with larger average values. In the tip area, higher total pressures are predicted at the flow region originated from the shroud suction surface corner but this is not so obvious in the experimental contours. At the exit plane of stator, Figure 19, quite similar total pressure contours are predicted as compared with the experimental ones, but with around 0.5 higher value in C_{pt} for most areas. In the areas between 5% to 80%, predicted total pressures increase from hub to tip and show maximum values at ahout 80% span, whereas in the experimental contours the total pressure is quite uniform. Obvious deficits (even larger in Model I) are predicted at the the flow region originated from the shroud suction surface corner that may due to the separation of the flow which does not appear in the experimental results.

Based on the above analysis, it is clear that the accuracy of the repeating stage boundary conditions is being assessed across the three spatial planes. Figure 5 and Figures 12 to 17 demonstrate the ability of the model to capture the axial flow variation. Figures 6 to 11 demonstrate the model's accuracy in the spanwise direction and Figures 18 and 19 demonstrate its accuracy in the tangential direction.

CONCLUSION

In the three-dimensional numerical simulation of multistage axial flow compressors,a steady state Navier-Stokes solver with non-uniform mixing plane model provides an accurate tool for the prediction of detailed internal flows and global aerodynamic performance.

In the prediction of the third stage of Cranfield Low Speed Research Compressor, the application of the proposed repeating stage model simplifies the definition of global aerodynamic boundary conditions so much that only mass flow rate and exit average static pressure are required for the prediction. The comparison between computational results and experimental data shows that the repeating stage model is an accurate and economical alternative to the expensive complete multistage simulations for the flow prediction in the rear stages of low pressure multistage axial flow compressors.

ACKNOWLEDGEMENT

The authors wish to thank the Laboratory of Thermal Turbomachines of the National Technical University of Athens for their kind permission to use "ELISA" at the initial phase of this project.

REFERENCES

Adamczyk, J.J., "Model Equation for Simulating Flows in Multistage Turbomachinery", NASA TM-86869; Also ASME paper, 85-GT-226, 1984.

Bolger, J.J. and Horlock, J.H., "Prediction of the Flows in Repeating Stages of Axial Flow Compressors Using Navier-Stokes Solvers", ASME Paper, 95-GT-199, 1995.

Chima, R.V., "Calculation of Multistage Turbomachinery Using Steady Characteristic Boundary Conditions", AIAA-98-0968, 1998.

Coons, S.A., "Surfaces for Computer Aided Design of Space Forms", MIT Report MAC-TR-41, 1967.

Dawes, W.N., "Toward Improved Throughflow Capability: The Use of Three-Dimensional Viscous Flow Solver in a Multistage Environment", *J. Turbomachinery*, Vol.114, pp.8-17, 1992.

Denton, J.D., "The Calculation of Three-Dimension Viscous Flow Through Multistage Turbomachineries", *J. Turbomachinery*, Vol.114, pp.18-26, 1992.

Faux, I.D. and Pratt, M.J., "Computational Geometry for Design and Manufacture", *Series: Mathematics and its Applications*, Ellis Horwood Publishers, 1979.

Howard, M.A., Ivey, P.C., Barton,J.P. and Young,K.F., "Endwall Effects at two Tip-Clearances in a Multistage Axial Flow Compressor with Controlled Diffusion Blading", *J. Turbomachinery*, Vol. 116, No.4, pp.635-647, 1994.

Launder, B.E. and Spalding, D.B., "The Numerical Computation of Turbulent Flows", *Int. Com. Meth. in Appl. Meth. Engg.*, Vol.3, pp.269-289, 1974.

LeJambre, C.R., Zacharias, R.M., Biederman, B.P., Gleixner, A.J. and Yetka, C.J., "Development and Application of a Multistage Navier-Stokes Flow Solver. Part II: Application to a High Pressure Compressor Design", ASME paper, 95-GT-343, 1995.

Leonard, B.P., "A Stable and Accurate Convective Modelling Procedure Based on Quadratic Upstream Interpolation", *Comp. Meth. Appl. Mech. Engg.*, Vol.19, pp.59-98, 1979.

Patankar, S.V. and Spalding, D.B., "A Calculation Procedure for Heat, Mass and Momentun Transfer in Three-Dimension Parabolic Flows", *Int. J. Heat Mass Transfer*, Vol.15, pp1787-1806, 1972.

Politis, E.S., Giannakoglou, K.C., and Papailiou, K.D., "Axial Compressor Stage Analysis Through a Multi-Block 3-D Navier-Stokes Solution Method", ASME Paper 97-GT-93, 1997.

Rai, M.M., "Unsteady Three-Dimensional Navier-Stokes Simulation of Turbine Rotor-Stator Interaction", *J. Propulsion and Power*, Vol.5, No.3, pp.307-319, 1989.

Rhie, C.M., Gleixner, A.J., Spear, D.A., Fischbery, C.J. and Zacharias, R.M., "Development and Application of a Multistage Navier-Stokes Solver. Part I: Multistage Modelling Using Bodyforce and Deterministic Stress", ASME paper, 95-GT-342, 1995.

Royle, R.J., and Giel, P.W., "Three-Dimensional Navier-Stokes Heat Transfer Predictions for Turbine Blade Rows", *J. Propulsion and Power*, Vol.11, No.6, pp. 1179-1186, 1995.

Stone, H.L., "Iterative Solution of Implicit Approximations of Multidimensional Partial Differential Equations", *SIAM J. Numerical Analysis*, Vol.5, pp.530-558, 1968.

Swoboda, M., Ivey, P.C., Wenger, U. and Gümmer, V., "An Experimental Examination of Cantilevered and Shrouded Stator in a Multistage Axial Compressor", ASME Paper, 98-GT-282, 1998.

Swoboda, M., Wenger, U., and Gümmer, V., "BRITE EURAM (Project AC3A) Blading Design Report for the 4-Stage CU(Cranfield University) Low Speed Research Compressor(LSRC)", Brite Euram Report 11-BRR-02, 1996.